Circuit Analysis and Design of Radial Pretuned Modules Used for Millimeter-Wave Oscillators

A. C. DERYCKE AND GEORGES SALMER

Abstract — **This paper summarizes the use of the radial pretuned module for the realization of millimeter-wave IMPATT or Gunn oscillators. Circuit analysis and derivation of an analytical model for the prediction of the characteristics of this type of oscillator are reviewed and the design of optimal structures is reported.**

Experimental results are also presented in order to justify the assumptions, which have been done to determine the range of validity of this model. This is done either by direct measurements or by the study of the behavior of millimeter-wave oscillators. Finally, we summarize the typical results obtained with this modular approach and its advantages versus classical ones.

I. Introduction

MANY MILLIMETER-WAVE applications need inexpensive and compact Gunn or IMPATT oscillators. The most classical solutions in this millimeter band are based on the cap structure or the Kurokawa structure [1], [2]. These structures give very good performances, especially for the characterization of nonencapsulated diodes [3], but they are not suitable for low-cost mass production. MIC's, on the other hand, present a strong case for the cost, the weight, the dimensions, and the automation of their productions.

Microstrips or suspended striplines are widely used for the realization of MIC's but meet with some problems above 50 GHz because the quartz substrate becomes very thin. Finline or E-plane circuits are other interesting and growing solutions for millimeter MIC's. But to our knowledge some problems remain: the biasing and the connection of the active device to the RF circuits is the first problem, the difficulty in getting a good thermal resistance is the second, and a low Q factor is the third.

The first problem is often solved by using standard packages. But the parasistic elements of these packages limit the RF performances and introduce sometimes unwanted frequency behavior. The second problem leads to the implementation of small holes in the substrate to access the ground plane and thermal dissipator.

Another means of overcoming these difficulties is to use pretuned modules (PTM's), which were proposed several years ago [4]–[6]. This modular approach has been used successfully over a wide range of frequencies (26 to 100 GHz) for Gunn and IMPATT devices. The purpose of this paper is devoted to the synthesis of our results and to the modeling and simulation of such a structure.

In the first part, we present a theoretical modeling of the pretuned module, which allows us to compute the evolution of the loading impedance "seen" by the active device as a function of frequency and of the size of the module.

In the second part, the theoretical model is compared with several experimental results of the direct measurement of this loading impedance to determine the validity range of the model.

In the third part, the model is used for the design of millimeter-wave oscillators. We present some rules for the design of optimum structures.

Finally, in the fourth part, a summary of the experimental results obtained for a millimeter-wave PTM is presented. These results show a good agreement with the theoretical predictions and exhibit some characteristics which justify the interest of such a structure.

II. Theoretical Analysis of the Pretuned Module

In this section, we present an analytical model for the determination of the loading impedance and its dependance on the geometrical dimensions of the module. This model must be easy to use for the design and mustn't be time consuming. These requirements exclude numerical models based on discretization. So we have chosen to establish a quasi-analytical formulation for the loading impedance. This yields some approximations. The major approximation is to consider that the pretuned module is located in free space on an infinite ground plane, and not placed in a rectangular waveguide. However, experimental studies on the coupling between the PTM and a rectangular waveguide have shown that the theoretical results are still valid in our case and that the use of such a model will be possible for optimization of oscillators with some care.

The electromagnetic system is described in Fig. 1, and it can be divided into two subsystems. This brings about two inter-dependant problems: 1) an interior problem (Region I) related to the propagation of waves between the two

Manuscript received October 10, 1983; revised February 11, 1985. This work was supported in part by the DRET and by the DAII.

The authors are with the Microwave and Semiconductor Center, L.A.C.N.R.S. no. 287, Université des Sciences et Techniques de Lille, 59655 Villeneuve D'ascq, Cedex, France.

0018-9480/85/0700-0600$01.00 ©1985 IEEE

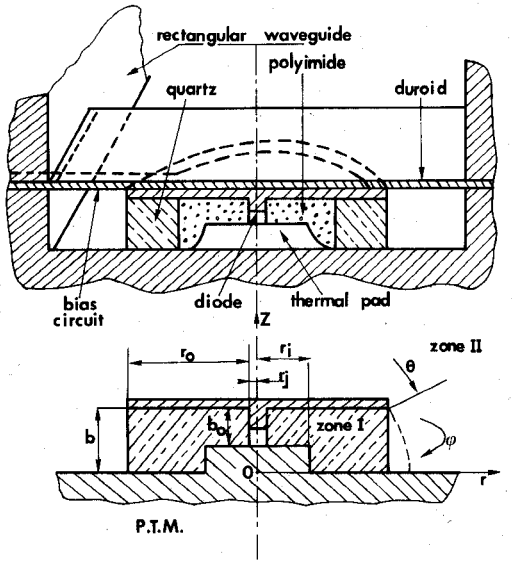

Fig. 1. The PTM configuration and the system of coordinates. Outer diameter = ϕ_o, inner diameter = ϕ_i.

metallic planes and 2) an exterior problem (Region II) related to the radiation of a circular slot.

In a classical way, the boundary conditions to be fulfilled by the fields on the aperture ($r = r_o$) give a relation between the two solutions for the fields in the two regions. It will be expressed by a radiation admittance Y_T located at $r = r_o$.

A. The Interior Problem (Region I)

1) The Radial Waveguide: This waveguide is nonuniform (the transverse section is varying along the propagation direction $\overline{Or}$). Our investigations are derived from Marcuvitz' works [7]. In the radial waveguide, the wave can be expressed as a superposition of TE and TM mode waves. These modes are not defined in relation with the $\overline{Or}$ propagation direction but in relation with the $\overline{Oz}$-axis.

TM modes must satisfy the boundary conditions ($E_z = 0$) at $z = 0$ and $z = b$. That gives the general relation

$$\psi_{mn} = E_0 \cos\left(\frac{n\pi}{b}\right) z \cdot \cos(m\varphi) \begin{Bmatrix} H_m^2(k_n r) \\ H_m^1(k_n r) \end{Bmatrix}. \quad (1)$$

TE modes: The wave functions are similar

$$\psi_{mn} = E_0 \sin\left(\frac{n\pi}{b}\right) z \cdot \cos(m\varphi) \begin{Bmatrix} H_m^2(k_n r) \\ H_m^1(k_n r) \end{Bmatrix}. \quad (2)$$

The subscripts m and n are relative to the φ and z coordinates, respectively, and $H_m^{1,2}(k_n r)$ are the Hankel functions of the first or second order which characterize the inward and outward waves, respectively, with

$$k_n = \sqrt{k^2 - \left(\frac{n\pi}{b}\right)^2} \quad \text{and} \quad k = \omega\sqrt{\mu_0 \epsilon}.$$

In practice, the optimum dimensions of the millimeter-wave PTM used for Gunn or IMPATT devices have such values that the following inequalities are always satisfied:

$$b/r_o < 1 \quad b/\lambda_o \ll 1.$$

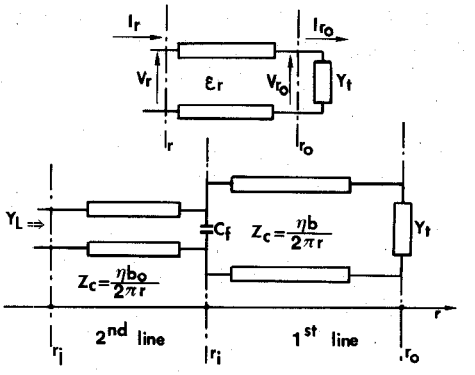

Fig. 2. Voltage and current conventions for a radial line and equivalent circuit for a real PTM.

In this case, for $n = 1$, the wavenumber k_n is an imaginary number ($k_n = j\alpha_n$) and the related modes must vanish very rapidly. For $n = 0$, only TM_{m0} has to be considered.

2) Equivalent Transmission Lines for the Radial Waveguide: The radial waveguide can be replaced by a nonuniform transmission line [7]. This is a generalization of the Marcuvitz treatment for all the TM_{m0} modes. Let us introduce two sets of auxiliary values V_m (pseudo-voltage) and I_m (pseudo-current). The electric and magnetic fields are tied to I_m and V_m by the following relations:

$$E_{zm} = -\frac{V_m}{b} \cdot \cos(m\varphi) \quad H_{\varphi_m} = \frac{I_m}{2\pi r} \cos(m\varphi) \quad (3)$$

where V_m and I_m are only functions of the r coordinate and V_m is a solution of

$$\frac{1}{r}\frac{d}{dr}\left(r\frac{dV_m}{dr}\right) + \gamma^2 V_m = 0 \quad (4)$$

where

$$\gamma^2 = k^2 - \left(\frac{m}{r}\right)^2.$$

The general solutions are Hankel functions

$$V_m = A_m H_m^2(kr) + B_m H_m^1(kr). \quad (5)$$

From these relations, we can derive a generalized transformation of the admittance between two values of r (r_o and r_i). The equivalent scheme is given by Fig. 2. If $I_m(r_o)$, $I_m(r_i)$, $V_m(r_o)$, $V_m(r_i)$ are the four values at $r = r_o$ and $r = r_i$, and if admittances are introduced with their definitions

$$Y(r_i) = \frac{I(r_i)}{V(r_i)} \quad Y(r_o) = \frac{I(r_o)}{V(r_o)}$$

then the following generalized admittance transformation is obtained:

$$Y(r_i) = \frac{1}{\gamma_i Z_i}\left[\frac{jk + \gamma_o Z_o Y(r_o) c_{tm}(x,y)\zeta_m(x,y)}{C_{tm}(x,y) + j\frac{\gamma_o Z_o}{k^2} \cdot Y(r_o)\zeta_m(x,y)}\right] \quad (6)$$

where C_{tm}, c_{tm}, and ζ_m are given in Appendix I, and where

$$\gamma_o^2 = k^2 - m^2/r_o^2, \quad Z_o = \frac{\eta b}{2\pi r_o} \cdot \frac{k}{\gamma_o}.$$

From studies of this generalized admittance transform, it appears that whatever the value of Y_m for the outer radius, for all the TM_{m0} modes ($m > 0$) the admittance $Y_m(r_i)$ tends to zero when $r_i \to 0$. This means that for centered active devices of small radius r_J, none of the higher modes could have a significant contribution to the loading impedance.

3) Equivalent Scheme for the Pretuned Module: From the above discussion, we can deduce an equivalent circuit for the pretuned module (Fig. 2). The load admittance seen by the active device of radius r_J will be calculated from the terminal admittance Y_T by means of the transform relation (6) applied successively to the two radial lines of height b and b_0, respectively. The discontinuity between the two radial lines can be taken into account by a capacitance C_f in parallel at $r = r_i$. This capacitance has a small influence and can be determined in a first approximation from a quasi-static model (modes TE_{0n} and TM_{0n} have no significant contribution).

4) Determination of Losses for the Fundamental Mode TM_{00}: For millimeter-wave operations of the PTM, it is important to evaluate the losses of such a structure and to keep them at a minimum level.

These losses are of two kinds: dielectric losses and metallic losses. The losses must be calculated for a stationary wave system established in the structure for which the ratio between outward and inward waves is related to the admittance Y_T. For this purpose, we have applied a perturbation method on the transmission-line formalism.

The lost power dP in a ring of width dr and radius r is given by the following relations.

In dielectric:

$$dP_d = \frac{\omega \epsilon tg(\delta) \cdot \pi \cdot r}{h} |V_{(r)}|^2 \, dr \tag{7}$$

where $t_g(\delta)$ is the loss tangent of the material and h the height of the considered radial line.

In metal:

$$dP_m = \frac{R_s}{2\pi} \frac{|I_{(r)}|^2}{r} \, dr \tag{8}$$

where $R_s = \sqrt{\frac{\pi \cdot F \cdot \mu}{\sigma_c}}$ is the surface resistivity.

The expression of P_m and P_d are given in Appendix II. The attenuation coefficient concept is meaningless in our case, so we have expressed the losses as a resistance R_P in series with the loading impedance

$$R_P = \frac{2(P_{d_1} + P_{d_2}) + 2(P_{m_1} + P_{m_2})}{|I(r_J)|^2} \tag{9}$$

where subscripts 1 and 2 are related to the two radial lines.

B. The Exterior Problem

The problem to be solved is the determination of the equivalent radiating admittance Y_T. To obtain Y_T, in real and imaginary parts, this determination must be achieved by a near-field approach to take into account the stored power near the aperture. For this purpose, the electromagnetic fields of the two regions are expressed in the form of a modal expansion. The application of the continuity equations between these fields at $r = r_o$ leads to the determination of the coupling factors and then to the admittance Y_T.

1) The Choice of the Modal Expansion:

a) Radial waveguide: Only the quasi-TEM mode is assumed to exist in the radial region (the higher modes of the same periodicity as the TEM mode, corresponding to $n \neq 0$ and $m = 0$, are far under their cutoff frequencies).

The two components of the electric fields are deduced from (1)

$$E_z^+(r) = \frac{E_o k^2}{j\omega\epsilon} \cdot H_0^2(kr)$$

$$H_\varphi^+(r) = -E_o k H_0^{2\prime}(kr) \tag{10}$$

and

$$Y_T = I(r_o)/V(r_o). \tag{11}$$

b) The exterior region: The real system presents such a geometry that the choice of a simple modal expansion is not easy. What is more difficult is to describe the fields above the structure in the vicinity of the metallic disc. We have chosen a modal expansion similar to that encountered for a spherical antenna [8] fed by a radial waveguide. We will introduce later a corrective term for the determination of Y_T to take into account the real structure. The electromagnetic fields are given by the following relations in the spherical coordinates (φ, θ, r):

$$rH_{\varphi_e} = \frac{1}{2\pi} \sum_{p=1,3,5} \frac{B_p}{p(p+1)} \cdot \frac{\hat{H}_p(k_0 r)}{\hat{H}_p(k_0 l_0)} \cdot \frac{d}{d\theta}\left(P_p \cos(\theta)\right) \tag{12}$$

$$rE_{\theta_e} = j\frac{\eta_0}{2\pi} \sum_{p=1,3,5} \frac{B_p}{p(p+1)} \cdot \frac{\hat{H}_p'(k_0 r)}{H_p'(k_0 l_0)} \cdot \frac{d}{d\theta}\left(P_p \cos(\theta)\right) \tag{13}$$

where $l_0 = r_0/\sin(\theta)$ and where η_0 and k_0 are the wave impedance and wavenumber, respectively, in region II, and

$$\hat{H}_p(k_0 r) = \left(\frac{\pi k_0}{2}\right)^{1/2} \left[J_{p+1/2}(k_0 r) - jY_{p+1/2}(k_0 r)\right]$$

is the spherical Hankel function, $\hat{H}_p'(k_0 r)$ its spatial derivative, and P_p the Legendre function of the pth order.

2) Determination of the Terminal Admittance Y_T:

a) The spherical model: To write the continuity equations at the interface between the two regions, we must express the fields on the cylindrical aperture at $r = r_o$.

In order to simplify the calculations, several assumptions can be introduced. The structure is chosen so that

$$b/\lambda_0 < 0.2 \quad b/r_o \ll 1$$

and

$$r_o/\sin(\theta) \simeq r_o.$$

The continuity equations can be written as

$$\int r_o H_\varphi^+(r_o)\, dz \simeq \int_{\overline{AB}} r_o H_{\varphi_e}(r_o)\, d\theta \tag{14}$$

and

$$E_z^+(r_o) \simeq E_{\theta e}(r_o).$$

By following a resolution method similar to that of Schelkunoff's [8], we can obtain

$$Y_T = \frac{\eta^2}{2Z_o^2\pi} \sum_{p=1,3,5} \frac{2(p+1)}{p(p+1)} Y_p^+ \left[P_p\left(\frac{b}{\sqrt{b^2+r_o^2}} \right) \right]^2 \tag{15}$$

where

$$Y_p^+ = \frac{-j\hat{H}_p(k_0 r_o)}{\eta_0 \hat{H}_p'(k_0 r_o)}$$

is the spherical wave admittance

b) Admittance Y_T of the PTM: The aforementioned expression for Y_T was obtained with the assumption that the upper part of the structure has a hemispherical geometry. A corrective term must then be introduced to obtain the admittance Y_T of the real structure. This is accomplished by introducing an excess capacitance C_Δ

$$Y_T' = Y_T + j\omega C_\Delta. \tag{16}$$

C_Δ is the difference of capacitance between the hemispherical cap and the circular disc cap, and is given by

$$C_\Delta = 4\epsilon_0 \cdot r_o \frac{\left[1 - \log\left(\pi - tg^{-1}(b/r_o)\right) + 0.52\right]}{\cos\left(tg^{-1}(b/r_o)\right)}.$$

We have used this value Y_T' in conjunction with the transform relations relative to the equivalent circuit. A computer program has been developed which is easy and fast to use (in practice only $p = 7$ or 9 spherical modes are enough to accurately describe the structure).

III. Experimental Check of the Model

We have performed some experiments to show the validity of the model and to determine its validity limits for the prediction of the characteristics of a PTM located inside a rectangular waveguide.

A. Measurements in Free Space

To compare our theoretical model with experimental results, we have made several structures using a scaling method down to the centimeter-wave range where the hardware is easier to make and systematic measurements are more accurate. The load impedance Z_L is measured over a wide frequency range (0.5–6 GHz) with an automatic network analyzer by substituting a small coaxial probe to the active device [9], for a PTM located in free space.

Fig. 3 is a comparison between theoretical and experimental results. The evolutions of the real and imaginary components of the load impedance are presented as a function of the electrical length kr_o. The frequency behavior of X_L presented in Fig. 3(a) is close to that of a single-mode resonant circuit (no TM_{m0} modes). The agreement between experiment and theory is good, especially for the range of X_L, which is of interest for operation of Gunn or IMPATT devices (where $5\ \Omega < -X_D < 40\ \Omega$).

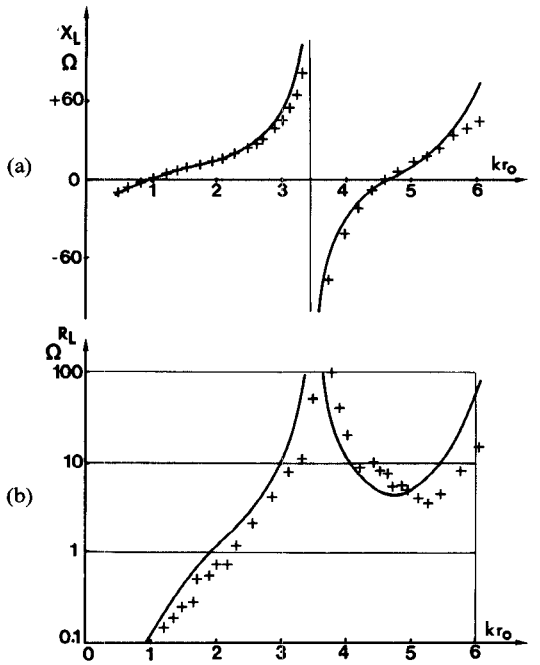

Fig. 3. Theoretical and measured values of the components of the load impedance versus kr_o, for a scaled down PTM. $\phi_o = 50$ mm, $\phi_i = 5$ mm, $b_0 = 1$ mm, $b = 3$ mm, $\phi_j = 1.3$ mm ($\epsilon_r = 4$ for quartz and $\epsilon_r = 3.8$ for polyimide).

The evolution of the load resistance R_L is presented in Fig. 3(b). A logarithmic scale was chosen to magnify the frequency behavior of the small resistance area, which is of interest for the realization of millimeter-wave oscillators.

Many comparisons have been performed for a wide range of geometrical sizes. They have allowed us to point out the validity range of the theoretical model. This is expressed by the following inequalities:

$$b/r_o < 1/5 \quad \text{and} \quad kr_o < 2.$$

The first limitation is mainly due to the approximations done for the derivation of Y_T. The second is probably in relation with the existence of vanishing higher TE_{n0} modes in the aperture for the highest frequencies.

B. Experimental Investigations of a PTM Located Inside a Rectangular Waveguide

Systematical measurements have been carried out for a PTM located inside a rectangular waveguide. In the first step, the waveguide is terminated at both ends by a matched load. The frequency behavior of the load impedance over the frequency range of the dominant TE_{10} waveguide mode is similar to the one measured or calculated for free space.

In the second step, one of the waveguide ends is terminated by a sliding short circuit. The locus of the load impedance at frequencies of practical interest versus the position of the sliding short circuit is then a circle very close to the calculated ones. However, some parasitic frequency resonances may appear if the exterior diameter

of the PTM is increased up to a value close to the waveguide width.

IV. Millimeter-Wave Oscillators Design

A. Some Important Features for the Realization of the Oscillators

The use of the computer program previously described gives the values of the load impedance and of the series resistance due to the PTM losses for each frequency. The oscillator design is fulfilled by an automatic search of the oscillator frequency for a given device.

If $X_D(F)$ is the frequency-dependent reactance of the considered diode, the oscillation frequency must satisfy the first oscillation condition, i.e.,

$$X_L(F_0)+X_D(F_0)=0. \tag{17}$$

For this frequency, F_0 (the second condition relative to the stability, as expressed by Kurokawa [10]) must also be satisfied. In order to simplify the computation, the active device is described by a simplified model.

The general expression of diode reactance is of the form

$$X_D=\frac{1}{C_{eq}\cdot 2\cdot\pi\cdot F^n}$$

where the equivalent capacitance C_{eq} is deduced from a computer simulation that we carried out for each doping profile, estimated surface, and bias current of such a device. The n power factor of F is approximated from these simulations (n goes from one to two). These simulations also give us the dependence of diode impedance versus the RF voltage, which is important to check the stability condition of the oscillator.

In this case, the computer program gives the oscillation frequency, the value of the load impedance (which will fix the value of generated power), the circuit efficiency, and the value of the loaded Q factor.

B. The Design of the Oscillators

We have systematically studied the dependence of the frequency of oscillation and load resistance as a function of geometrical dimensions of the PTM.

1) External Diameter ($\phi_o = 2\cdot r_o$): This external diameter is an important parameter as can be seen in Fig. 4. The frequency of oscillation is inversely proportional to ϕ_o for all the values of the diode area.

The load resistance is nearly constant with ϕ_o (Fig. 4) or slowly decreasing, especially in the small diameter range. This is confirmed by measurements achieved by Doring and Seebald [11] for a classical cap structure in a rectangular waveguide.

2) Height b: The frequency of oscillation presents only smooth variations when b is varied, approximately like a $b^{-0.4}$ law, as shown in Fig. 5. On the other hand, the load resistance is a nearly linear function of b in the mid-range (Fig. 6). These results are also confirmed by previous authors [11], [12]. Several experimental and theoretical studies have shown that for IMPATT or Gunn diodes, the empirical law describing the dependence of the frequency of oscillation varies from $b^{-0.4}$ to $b^{-0.6}$.

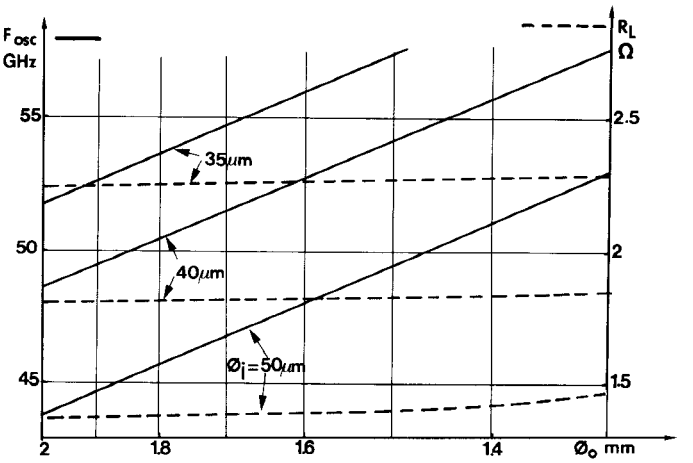

Fig. 4. Oscillation frequency and load resistance versus outer diameter ϕ_o for IMPATT DSR diode of various junction diameters ϕ_j. $b=150$ μm, $b_0=50$ μm, $\phi_i=160$ μm.

3) The Interior Diameter: ϕ_i also has an important influence (Fig. 7) on the oscillation frequency, and the load resistance is proportional to ϕ_i in the considered range.

4) The height b_0: at the vicinity of the diode is also an important parameter, especially for the load resistance. However, some technological limitations do not allow the use of these dimensions as tuning elements.

In each frequency range of operations, we have deduced from the theoretical results some analytical laws. They can readily provide an estimation of the frequency of oscillation and load resistance relative to a set of dimensions.

For example, for the IMPATT SDR diodes in the 40–60-GHz range

$$F_0(GHz)=\frac{30.9}{\phi_o}+\frac{94}{b^{0.4}}+75\phi_i+\frac{0.86}{\phi_J}-20$$

$$R_L(\Omega)=12.5b+2\phi_i+\frac{0.01}{\phi_J^{1.6}}-2.1$$

where $\phi_J=2r_J$ is the diode diameter, b_0 is a constant, and all the dimensions are in millimeters. These laws are valid for

$$1.3\leqslant\phi_o\leqslant 2 \quad 0.12\leqslant b\leqslant 0.2 \quad 0.1\leqslant\phi_i\leqslant 0.2$$

$$30\leqslant\phi_j\leqslant 50\ \mu\text{m}$$

and for the IMPATT SDR with an optimal doping profile.

Remarks

1) In the case of Gunn diodes, it is of interest to specify the limit of operation when the ratio X_L/R_L becomes too small. It has been shown that this limit is such that this ratio is always greater than one.

2) The load resistance at the oscillation frequency must be equal to its optimal value to obtain the maximum RF power. This value depends on the diode area and varies from ϕ_J^{-3} for low bias currents to ϕ_J^{-2} from higher currents. In the proposed example, the dependence is close to

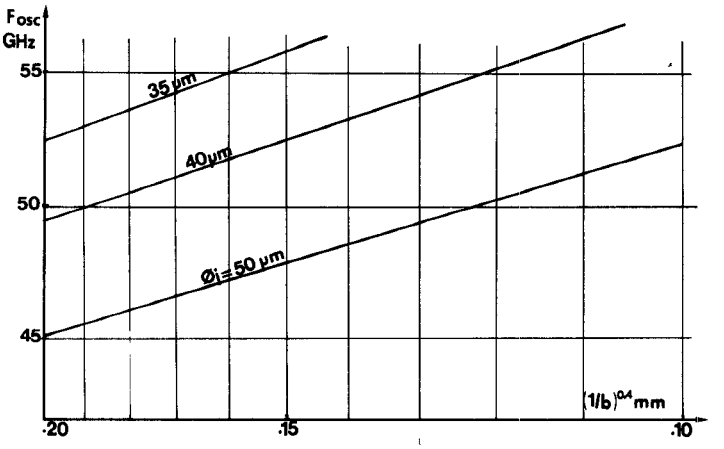

Fig. 5. Frequency of oscillation versus a $b^{-0.4}$. $b_0 = 50$ μm, $\phi_i = 160$ μm, $\phi_o = 1.6$ mm.

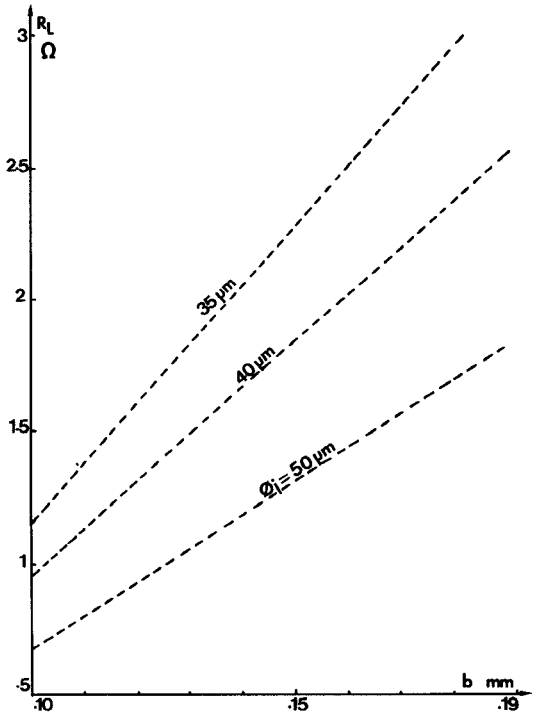

Fig. 6. Load resistance R_L versus height b (same conditions as in Fig. 5).

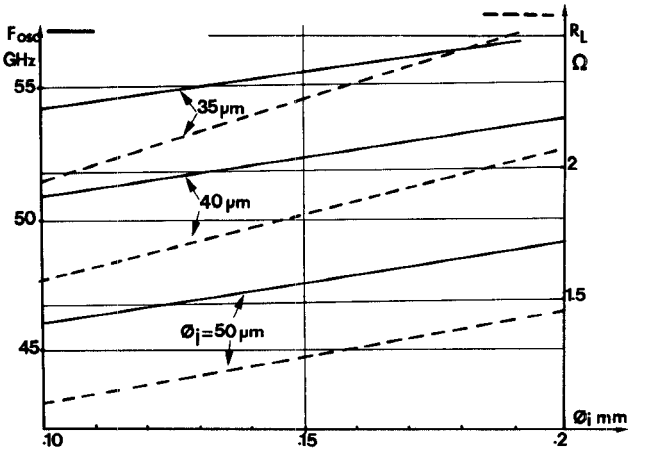

Fig. 7. Oscillation frequency and load resistance versus interior diameter ϕ_i. $\phi_o = 1.6$ mm, $b = 150$ μm.

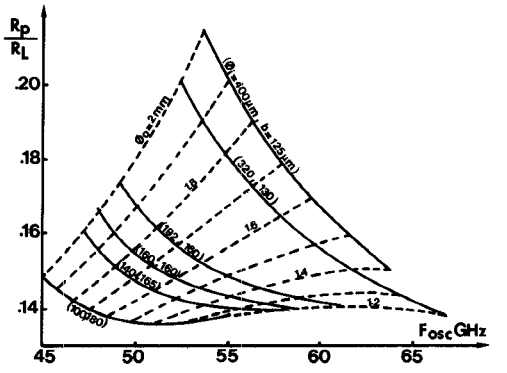

Fig. 8. Dependence of circuit losses versus frequency of oscillation with circuit dimensions as parameters with given load resistance $R_L = 2$ Ω. $b_0 = 50$ μm, $\sigma_c = 10^7$ mho/cm, $tg\delta_1 = 0.001$, $tg\delta_2 = 0.01$ (σ_c for sputtered gold, $tg\delta_1$ and $tg\delta_2$ are the loss tangents for quartz and polyimide).

$\phi_J^{-1.6}$. The optimization will then be valid for only a relatively narrow range of junction diameters.

C. Some General Rules for the Design of the PTM

At first look, the operation characteristics depend on five main parameters ($\phi_J, \phi_i, \phi_o, b, b_0$). In practice, b_0 is imposed by technological constraints and it is difficult to adjust. The junction diameter is imposed by the power level requirement or by the maximum dc power which must be dissipated.

Three parameters are then used to search the optimal conditions of operation. These parameters must satisfy the oscillation conditions and the optimal value of the load resistance R_L.

There exists an infinite number of possible sets of dimensions. So we must choose the values which provide the minimum circuit losses and the highest loaded Q factor. From the examination of Figs. 8 and 9, it appears that, for an imposed frequency, the exterior and interior diameters must be as small as possible, while b must be as large as possible in the limits of the technological feasibility.

The circuit efficiency is better for a Gunn diode because the optimal values of the load resistance are generally higher than those met for the IMPATT SDR.

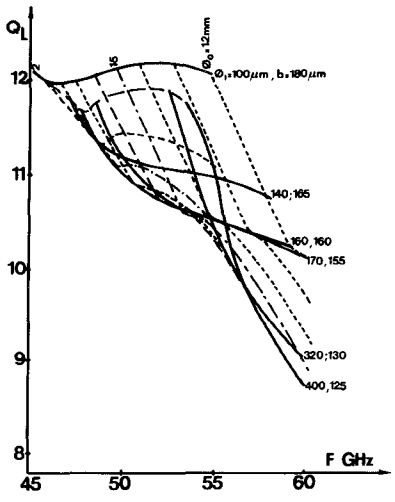

Fig. 9. Dependence of the loading Q factor versus frequency of oscillation for various ϕ_i, b, ϕ_o parameters (same conditions as in Fig. 8).

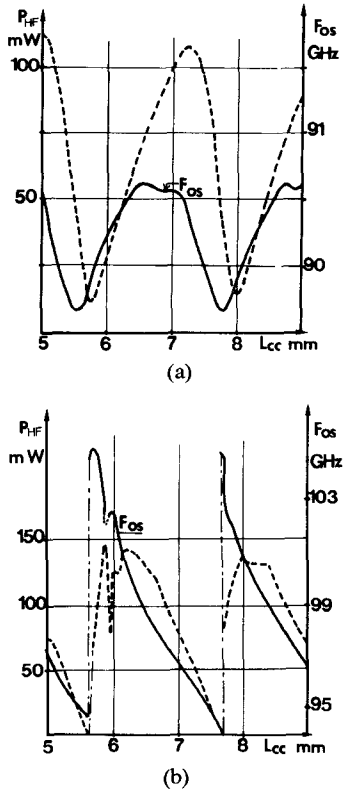

Fig. 10. RF power and oscillator frequency versus sliding short-circuit position (a) for a PTM and (b) for a standard package. IMPATT diodes are issue of the same batch.

V. Synthesis of Experimental Results of PTM Oscillators in the Millimeter-Wave Range

Several PTM's have been made from two different technological processes: either in the form of a "super device" [4], or in the form of planar circuits similar to those described by Sicking [13]. These PTM's have been designed with IMPATT (single or double drift) or Gunn diodes for operation in the R (26–40-GHz) to W (75–100-GHz) frequency ranges. From numerous experiments, we have established a correlation between theory and practice which has justified our approach.

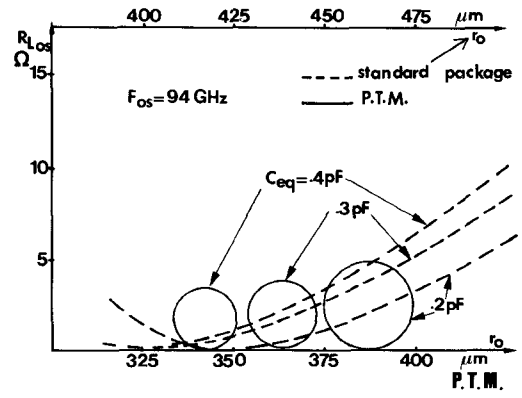

Fig. 11. Locus of the load resistance and required outer diameter with sliding short position as parameter (a) for a PTM with an active device of various equivalent capacitances and (b) for a standard package with the same device.

A. Mode of Operation of a PTM Oscillator Located in a Rectangular Waveguide

The fundamental assumption for the model (i.e., free-space radiation) has already been justified by direct measurement in the centimeter-wave range. The study of millimeter-wave oscillator tuning has also confirmed our choice. The mechanical tuning range achieved with the sliding short is narrow (only a few percent), and tuning for maximum power was shown to be smooth and easily reproducible. Fig. 10 gives an example of the power and frequency dependence versus the sliding-short position for quasi-identical diodes located either in a standard package (W3) (Fig. 10(b)) or in a PTM (Fig. 10(a)) and operated in a similar waveguide test fixture.

In the PTM case, the dependences of P_{RF} and F_o are regular and close to the classical dependences following a $\sin^2(\beta_g L_{cc})$ law for the power and a $\sin(2\beta_g L_{cc})$ law for the frequency which corresponds to the modulation of R_L and X_L due to the variation of the sliding-short position. If the waveguide is terminated by two matched loads, the oscillator still works and the generated output power and frequency are of the same order as those obtained with a sliding short.

In the standard package case, the power and frequency behavior are quite different. The dependence of frequency is larger than in the PTM case, and the mode of operation is close to a rectangular cavity one (Fig. 10(b)).

Another way to justify the interest in the PTM versus the standard package is illustrated in Fig. 11. This figure shows the theoretical value of the load resistance which can be achieved for a given frequency (i.e., 94 GHz) and a known diode capacitance by mechanical tuning and adjustment of the external diameter (ϕ_o). For the PTM, we obtain some small circles which point out that the possible range of ϕ_o is limited for a given device (hence, the name of pretuned module). On the contrary, for a standard package, the

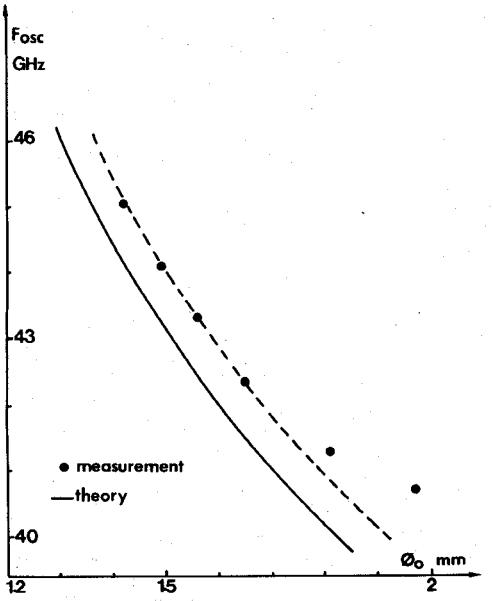

Fig. 12. Theoretical and experimental dependences of the frequency of oscillation versus outer diameter for an IMPATT SDR diode PTM. $\phi_i = 200\ \mu m$, $b_0 = 90\ \mu m$, $b = 193\ \mu m$.

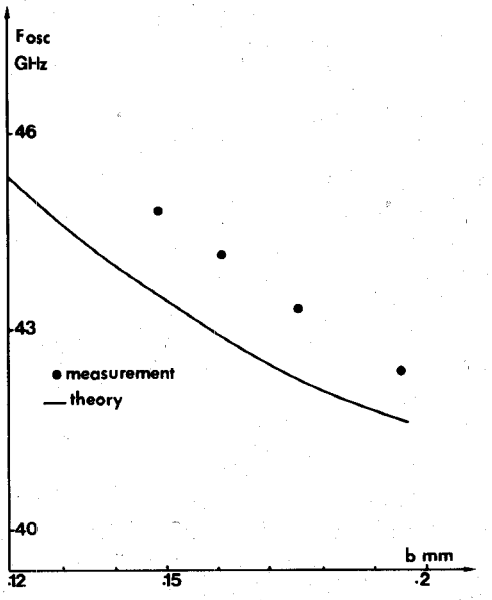

Fig. 13. Theoretical and experimental dependences of the frequency of oscillation versus the height b, for an IMPATT SDR diode PTM. $\phi_i = 200\ \mu m$, $b_0 = 103\ \mu m$, $\phi_o = 1.65$ mm.

range of the possible values of R_L is very wide and, besides, the values of the diode capacitance are not critical.

B. Comparison Between Theory, Design, and Experimental Results

In the millimeter-wave range, the exact correlation between theory and experiment is not an easy task. Indeed, some parameters which are introduced in the computer program cannot be accurately determined. In our case, the problem is linked with the technological dispersion which introduces some uncertainties on the device reactance and its exact dependance with the dc bias current, as well as on the dimensions of the radial structure in the vicinity of the diode (value of b_0).

In order to make a correlation between theoretical and experimental results, we have studied mainly the relative dependence of the frequency of oscillation as a function of ϕ_o and b, and to overcome the aforementioned problems, we have always used the same diode.

The different values of ϕ_o were obtained by successive etching of the upper metallization. The corresponding results are presented in Fig. 12. For the study of the influence of b, the same module was successively overlapped and remetallized (the results are reported in Fig. 13). From these comparisons, it appears that the oscillation frequency follows a ϕ_o^{-1} law for both theory and experiment, except for the large values for which the experimental decrease is slower. This is probably due to the waveguide sidewall effects on the PTM which are not taken into account in this model. On the other hand, the theoretical and experimental evolutions of the oscillation frequency versus b are quite similar (a $b^{-0.4}$ law).

TABLE I

Characteristics / Device	Fosc. GHz	ϕ_o mm	b mm	P_{HF} mW
Impatt SDR	30	4,5	0,3	500-700 (3W)*
Impatt SDR	50	2	0,2	300
Impatt SDR	94	1	0,1	150-200
Impatt DDR	94	1,1	0,12	300-400 (800)*
Gunn	35	1,8	0,5	200

Mean characteristics of various PTM for a junction temperature $T_j < 200°$ C.
* State of the arts results for Silicon DDR Impatt diode on diamond heatsink [16]

The discrepancy between theory and experiment are of the order of a few percent and it can rise to ten percent in the worst cases. However, we have noted that this error always follows the same trend: the experimental values of the frequency are always higher.

C. Summary of Experimental Results for the PTM

We summarize in Table I the mean results obtained in three frequency ranges with three kinds of active devices [4], [14].

These results must be compared to those obtained with standard packaging for frequencies below 60 GHz. For these frequency ranges, the power levels are of the same order for diodes coming from the same batch. On the other hand, PTM's present some advantages.

1) The thermal frequency stability is increased as compared with the standard package in a noncompensated

cavity (for example, $\Delta F_0/F_0 = 4.10-5/°C$ for a PTM Gunn oscillator at 40 GHz).

2) The dependence of the RF power versus bias current are more regular (no hysterisis or power or frequency jumps). This is probably due to the fact that in the PTM, the matching circuit is nearly located in the immediate vicinity of the diode.

For frequencies above 60 GHz, the results obtained with the PTM must be compared with those obtained with unpackaged diodes. In this case, the PTM output power is always 1 to 2 dB below the power obtained for the unpackaged diodes. However, this last solution is not well suited for practical applications.

VI. Conclusion

The use of PTM's is interesting in the millimeter-wave range for the realization of IMPATT or Gunn diode oscillators. The approximated analytical model presented here allows a better design of such a structure, in order to obtain optimal characteristics of the oscillators.

Different realizations between 40 to 100 GHz have shown that PTM's have also some interesting features for system applications of millimeter-wave IMPATT sources. The most important features are: mechanical ruggedness of this setup, monotonic dependence of RF power versus bias current, and smoothness of mechanical tuning.

We have also used this approach for the realization of voltage-controlled oscillators which have an associated varactor diode and a Gunn diode inside the same module for the *Ka*-band [15]. The PTM approach is also investigated for a power combiner which adds the power of four to six IMPATT diodes in the 94-GHz frequency range.

Appendix I

$$C_{sm}(x,y) = \frac{-J'_m(y)Y_m(x)+Y'_m(y)J_m(x)}{U}$$

$$c_{sm}(x,y) = \frac{J_m(y)Y'_m(x)-Y_m(x)J'_m(x)}{U}$$

$$S_{nm}(x,y) = \frac{Y'_m(y)J'_m(x)-J'_m(y)Y'_m(x)}{U}$$

$$s_{nm}(x,y) = \frac{J_m(y)Y_m(x)-Y_m(y)J_m(x)}{U}$$

where

$$U = \frac{2}{\pi y} \quad x = kr_i \quad y = kr_o$$

and where I_m, Y_m, I'_m, and Y'_m are Bessel functions of the first and second kind, and their derivatives are

$$c_{tm}(x,y) = \frac{c_{sm}(x,y)}{-s_{nm}(x,y)}$$

$$C_{tm}(x,y) = \frac{C_{sm}(x,y)}{S_{nm}(x,y)}$$

$$\zeta_m(x,y) = \frac{s_{nm}(x,y)}{S_{nm}(x,y)}.$$

Appendix II
Dielectric Losses

The power lost into the radial line of height b is

$$P_d = \int_{r_i}^{r_o} dP_d = \frac{\sigma_d \pi}{b} \int_{r_i}^{r_o} |V(r)|^2 \cdot r \cdot dr$$

$$\sigma_d = \omega \epsilon tg(\delta).$$

We can express the voltage on the r-axis as a function of the voltage and the admittance Y_T at the r_o-axis. This yields

$$V(r) = V(r_o) \cdot \left[C_{sm}(\alpha, y) + Z_o B_T s_{nm}(\alpha, y) - jZ_o G_T s_{nm}(\alpha, y)\right]$$

where

$$Y_T = G_T + jB_T$$

$$\alpha = kr \quad y = kr_o.$$

The report of $V_{(r)}$ into the A-1 relation gives

$$P_d = \frac{\sigma_d \cdot \pi}{b} \int_{r_i}^{r_o} |V_{(r)}|^2 \left[C_{sm}(\alpha, y) + Z_o^2 |Y_T|^2 s_{nm}(\alpha, y) + 2Z_o B_T s_{nm}(\alpha, y) C_{sm}(\alpha, y)\right] \cdot r \cdot dr.$$

This gives some Lommel integral defined as

$$A_p = \int_{r_i}^{r_o} r \cdot J_p^2(\alpha)\, dr \quad B_p = \int_{r_i}^{r_o} Y_p^2(\alpha)\, dr$$

$$C_p = \int_{r_i}^{r_o} r J_p(\alpha) Y_p(\alpha)\, dr, \qquad p = 0, 1.$$

The expression of P_d is then

$$P_d = \frac{\sigma_d \pi}{b} \cdot \frac{\pi^2 y^2}{4} \left[D_0(r_i, r_o) + Z_o^2 |Y_T|^2 E_0(r_i, r_o) + 2Z_0 B_T F_0(r_i, r_o)\right] \cdot |V(r_o)|^2$$

where D_0, E_0, F_0 are given by (with $p = 0$)

$$D_p(r_i, r_o) = A_p Y_1^2(y) + B_p \cdot J_1^2(y) - 2C_p \cdot J_1(y) Y_1(y)$$

$$E_p(r_i, r_o) = A_p Y_o^2(y) + B_p \cdot J_0^2(y) - 2C_p \cdot J_0(y) Y_0(y)$$

$$F_p(r_i, r_o) = A_p Y_0(y) Y_1(y) + B_p J_0(y) J_1(y) - 2C_p (J_1(y) Y_0(y) - J_0(y) Y_1(y)).$$

We can express the losses under the form of a series resistance located at the r_i position

$$R_{Pd} = \frac{2P_d}{|I(r_i)|^2} = \frac{2P_d Z_i^2}{|V(r_{(i)})|^2}$$

where

$$Z_i = \frac{\eta b}{2\pi r_i}.$$

The metallic losses are calculated in the same way

$$P_m = \frac{R_s}{2\pi} \int_{r_i}^{r_o} |I_{(r)}|^2 \frac{dr}{r}$$

where R_s is the surface resistivity.

The calculation leads to

$$P_m = \frac{\pi^3 R_s y^2}{\eta^2 b^2 \cdot 2}\left[D_1(r_i, r_o) + Z_o^2 \cdot |Y_T|^2 \cdot E_1(r_i, r_o) + 2B_T Z_o F_1(r_i, r_o)\right]|V_{(r_o)}|^2.$$

The expressions of D_1, E_1, F_1 are given by aforementioned relations with $p = 1$. The series resistance is given by

$$R_{pm} = \frac{2Pm}{|I(r_i)|^2}.$$

Acknowledgment

The authors acknowledge the contributions of G. Cachier, L. Dupont, M. Dejeager, A. Debouard, J. Espaignol, and R. Funck for the PTM realization, the processing of IMPATT and Gunn devices, and for the oscillator characterization and evaluation.

References

[1] I. S. Groves and P. E. Lewis, "Resonant cap structures for IMPATT diodes," *Electron. Lett.*, vol. 8, pp. 98–99, Feb. 1972.
[2] F. M. Magalahaes and K. Kurokawa, "A single tuned oscillator for IMPATT characterizations," *Proc. IEEE*, pp. 831–832, May 1970.
[3] T. A. Midford and R. L. Bernick, "Millimeter-wave c.w. IMPATT diodes and oscillators," *IEEE Trans. Microwave Theory Tech.*, vol. MTT-27, pp. 483–491, May 1979.
[4] G. Cachier, J. Espaignol, and J. Stevance, "Millimeter-wave pretuned mocules," *IEEE Trans. Microwave Theory Tech.*, vol. MTT-27, pp. 505–510, May 1979.
[5] G. Cachier and J. Stevance, "Modular techniques for controlling the frequency of millimeter IMPATT's," in *Proc. ISSCC* 79, Feb. 1979, pp. 170–171.
[6] A. C. Derycke, L. Dupont, M. del Guidice, and G. Salmer, "An accurate broadband desktop computer modeling for radial integrated microwave circuits," in *Proc. EUMC*, (Paris), pp. 116–120.
[7] N. Marcuvitz, *Waveguide Handbook* (Radiation Lab. Series). New York: McGraw-Hill, 1951.
[8] S. A. Schelkunoff, *Advanced Antenna Theory*. New York: Wiley, 1952.
[9] R. L. Eisenhart and P. J. Khan, "Theoretical and experimental analysis of waveguide mounting structure," *IEEE Trans. Microwave Theory Tech.*, vol. MTT-19, pp. 706–719, Aug. 1971.
[10] K. Kurokawa, "Some basic characteristics of broadband negative resistance oscillator circuits," *Bell Syst. Tech. J.*, pp. 1937–1955, July/Aug. 1969.
[11] K. H. Doring and E. Seebald, "High transformation ratio for impedance matching with a radial line," *Electron. Lett.*, vol. 16, no. 2, pp. 50–51, Jan. 17, 1980.
[12] K. H. Doring and E. Seebald, Deutsche Post Tech. Rep., private communication.
[13] F. Sitking and H. Meinel, "Multidiode *Ka*-band oscillators using hybrid planar circuit design," in *Proc. MTT Symp.*, 1981, pp. 62–64.
[14] M. Heitzmann and M. Boudot, "New progress in a development of a 94-GHz pretuned module silicon IMPATT diode," *IEEE Trans. Electron Devices*, vol. ED-30, pp. 759–763, July 1983.
[15] A. Derycke, M. Dejeager, G. Salmer, and A. Debouard, "Experimental and theoretical investigations of radial microwave integrated circuits multi-semi conductor devices," in *Proc. 10th E.U.M.C.*, (Varsovy), Sept. 1980, pp. 608–612.
[16] Y. Ma, M. Simonuti, and H. Yen, "Recent advances in millimeter-wave IMPATT sources," Hughes Aircraft Co., private communications.

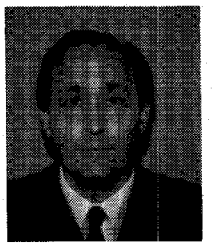

A. C. Derycke was born in Cappelle la Grande, France, on August 15, 1947. He received the doctor of third cycle degree in electronics from the University of Sciences and Technics of Lille, France, in 1975.

Since 1972, he has been a member of the Centre Hyperfréquence et Semiconducteurs Laboratory of this University, where his research interest has been the GaAs IMPATT diode, its use in frequency multiplication, and the millimeter-wave generator (v.c.o, combine, MIC's). He is presently interested in monolithic circuits and patch antennas for millimeter waves.

As Associate Professor, he is currently Head of the Department for Computer Sciences and Electrical Engineering in Further Education, where he directs works on computer-assisted instruction and educational uses of local area networks.

Georges Salmer was born in Besançon, France, on August 7, 1939. He received the Dipl. Eng. degree from the Institut Supérieur d'Electronique du Nord, Lille, France, and the Doctorat ès Sciences Physiques degree from the University of Lille, Lille, France, in 1961 and 1966, respectively.

He joined the Centre Hyperfréquences et Semiconducteurs, University of Lille I, Villeneuve d'Ascq, France, in 1968. Currently, he is a Professor at the University of Lille and group leader at the center. He is working on microwave solid-state devices, mainly on device modeling and characterization. At the beginning, he was studying IMPATT and BARITT devices, especially high-efficiency Read and high–low GaAs devices. Since 1977, he has worked on low-noise and power submicronic GaAs MESFET's and TEGFET's.